0026-895X/91/050742-08$03.00/0

MOLECULAR PHARMACOLOGY, 40:742-749

ω-Conotoxin Exerts Functionally Distinct Low and High Affinity Effects in the Neuronal Cell Line NG108-15

JOHN L. WERTH, LANE D. HIRNING, and STANLEY A. THAYER

Department of Pharmacology, University of Minnesota Medical School, Minneapolis, Minnesota 55455 (J.L.W., S.A.T.), and Natural Product Sciences, Salt Lake City, Utah 84108 (L.D.H.)

Received January 28, 1991; Accepted July 23, 1991

SUMMARY

The Ca^{2+} channel blockade produced by ω-conotoxin GVIA (ω-CgTx) was studied in single, forskolin-differentiated, NG108-15 cells, using dual-emission microfluorimetry and the whole-cell patch-clamp technique. Whole-cell currents through Ca^{2+} channels were measured with 5 mM Ba^{2+} as the charge carrier. Application of 1 μM nitrendipine inhibited by 90% the currents evoked by stepping from −30 mV to 0 mV. ω-CgTx (1 μM) inhibited these currents by 28%. These data suggest the possibility that NG108-15 cells express two types of dihydropyridine-sensitive Ca^{2+} channel, one sensitive and the other insensitive to blockade by ω-CgTx. The nature of the Ca^{2+} channel blockade produced by these agents was studied further, using depolarization-induced intracellular free Ca^{2+} concentration ($[Ca^{2+}]_i$) transients recorded with the Ca^{2+} indicator indo-1 and a dual-emission microfluorimeter. A 30-sec superfusion with 50 mM K^+ increased the $[Ca^{2+}]_i$ from a basal level of 142 ± 10 nM to a peak level of 1655 ± 287 nM. This $[Ca^{2+}]_i$ transient was blocked completely and reversibly by nitrendipine, in a concentration-dependent manner (IC_{50} = 1.9 nM). In contrast, ω-CgTx produced a maximal inhibition of the depolarization-induced rise in $[Ca^{2+}]_i$ of only 52% in the presence of physiological concentrations of divalent metals. The block was irreversible. This inhibition was concentration dependent until the point of maximal inhibition, at which point the channel block reversed in a graded manner. This entire U-shaped dose-response curve could be shifted in a parallel fashion by modulation of the extracellular divalent metal concentration, without changes in the maximal inhibition. Repeated applications of or prolonged incubations with ω-CgTx failed to increase the maximal block. Treatment with a high (1 μM) concentration of ω-CgTx, which produced a modest (10%) inhibition of Ca^{2+} influx, protected the cell from a second exposure to a normally effective concentration of ω-CgTx (10 nM). Depolarization-induced $[Ca^{2+}]_i$ transients in cells treated with 10 nM toxin were inhibited by 45%, and this inhibition could not be reversed by subsequent exposure to a high concentration of ω-CgTx. We conclude that there are two ω-CgTx binding sites on these cells, one to which ω-CgTx binds with high affinity, producing an irreversible Ca^{2+} channel blockade, and a second to which ω-CgTx binds with lower affinity. Binding to this second site is irreversible and does not block the channel but does prevent access to the high affinity site. These data suggest caution in the use of ω-CgTx as a tool to distinguish Ca^{2+} channel subtypes.

Voltage-sensitive Ca^{2+} channels serve the dual purpose of carrying charge during the neuronal action potential and transducing this electrical signal into a chemical message, represented by a rise in the $[Ca^{2+}]_i$ (1). There are multiple types of Ca^{2+} channels (2), of which at least four, designated T, N, L, and P, have been described in neurons (3–6). Ca^{2+} channel subtypes can be distinguished on the basis of their unitary conductance, voltage dependence of activation, and kinetics of inactivation. There has been great interest in the development of drugs that act specifically at these different channel types. However, to date only agents selective for the L-type Ca^{2+} channel have been developed, of which the dihydropyridine drugs are the most potent. Less potent agents have been reported to act at T-type channels (7). Peptide toxins such as ω-CgTx and calciseptin are the only naturally occurring agents known to act at mammalian Ca^{2+} channels (8, 9) (but also see Ref. 10). ω-CgTx will potently inhibit both the N- and L-type channels found in chick dorsal root ganglion neurons (11). However, recent reports suggest that L-type Ca^{2+} channels may be insensitive to or inhibited only transiently by ω-CgTx (12, 13).

The discovery of multiple Ca^{2+} channel subtypes led to the search for specific functions linked to identified channel subtypes. In sympathetic neurons the depolarization-evoked release of [^{3}H]norepinephrine is mediated by N-type Ca^{2+} chan-

This work was supported by Grant DA06781 from the United States Public Health Service and Grant BNS9010486 from the National Science Foundation and, in part, by the American Heart Association, the Joseph P. Kennedy Foundation, the University of Minnesota, and ICI Americas, Inc. (S.A.T.). J.L.W. was supported by grant T32DA07097 from the National Institute on Drug Abuse.

ABBREVIATIONS: $[Ca^{2+}]_i$, intracellular free Ca^{2+} concentration; ω-CgTx, ω-conotoxin GVIA; HEPES, 4-(2-hydroxyethyl)-1-piperazineethanesulfonic acid; EGTA, ethylene glycol bis(β-aminoethyl ether)-*N,N,N′,N′*-tetraacetic acid; TEA, tetraethylammonium.

nels (14). In contrast, in sensory neurons the depolarization-evoked release of substance P is mediated by dihydropyridine-sensitive channels and is, thus, presumed to involve L-type Ca^{2+} channels (15, 16). In cerebellar olive neurons it appears that a heterogeneous spatial distribution of a low voltage-activated Ca^{2+} channel, analogous to the T-type channel, is responsible for the pacemaking activity that originates in the dendrites of these cells (17, 18). Not only can specific functions be ascribed to particular channel subtypes, but Ca^{2+} channels also exhibit tissue-specific pharmacological properties. This is illustrated by the selective inhibition by ω-CgTx of Ca^{2+} currents in neurons, whereas it spares Ca^{2+} channels present in muscle cells (8, 19). Clearly, functional and tissue specificity make Ca^{2+} channel subtypes promising pharmacological targets.

In this report, we describe experiments designed to determine pharmacologically the Ca^{2+} channel subtypes that mediate depolarization-induced $[Ca^{2+}]_i$ transients in the neuronal cell line NG108-15. Using ω-CgTx as a pharmacological tool, we were surprised to find that the toxin produced a U-shaped dose-response curve. The possibility that this curve is the result of two functionally distinct ω-CgTx binding sites is discussed.

Materials and Methods

Cell culture. NG108-15 cells (passages 24–30) were grown in culture as previously described (20). Briefly, cells were plated onto glass coverslips (25-mm, round), at a density of 3×10^4 cells/coverslip, and were maintained in Dulbecco's modified Eagles medium supplemented with 5% fetal bovine serum, 0.1 μM hypoxanthine, 10 μM aminopterine, and 17 μM thymidine, in a humidified atmosphere of 95% air/5% CO_2 at 37°. After 1–2 days in growth medium, cells were placed in serum-free medium containing 5 μM forskolin, to induce cellular differentiation. Cells were used after 5–6 days in differentiating medium.

Ca^{2+} current recordings. The whole-cell configuration of the patch-clamp technique (21) was used to record calcium currents from single cells. The coverslips on which the cells were grown were placed in a perfusion chamber on an inverted microscope. The patch pipet contained an internal solution of (in mM) $CsCl_2$, 100; EGTA, 10; HEPES, 40; Mg^{2+}, 0.5; ATP, 2; and GTP, 0.35; pH 7.35. The superfusion solution was a 5 mM Ca^{2+}-Tyrode's solution composed of (in mM) Na^+, 126; K^+, 5; HEPES, 10; glucose, 10; and Mg^{2+}, 1; pH 7.35. The gigaseal was formed in this solution, and the cell membrane at the pipette tip was ruptured by suction to allow whole-cell voltage clamp. The presence of a fast inward Na^+ current was a requirement for recording currents from a cell and was taken as an indicator of a viable cell. The perfusate was then changed to a Na^+-free solution containing 5 mM Ba^{2+} and (in mM) TEA-Cl, 135; HEPES, 10; and glucose, 10; pH 7.35; with 1 μM tetrodotoxin. Using Ba^{2+} as the charge carrier enhanced the magnitude of the currents and, consequently, our ability to resolve them. Internal and external ionic solutions were chosen to isolate Ca^{2+} currents from other currents. Inward Na^+ current was eliminated by substitution of TEA for Na^+, and K^+ currents were eliminated by using internal Cs^+ and external TEA and Ba^{2+}. Ca^{2+}-activated currents, as well as Ca^{2+}-induced inactivation of calcium currents, were suppressed by 10 mM EGTA in the internal solution. Ca^{2+} currents were elicited by 200-msec depolarizations, at intervals of 5–10 sec, from a −30 mV holding potential.

The currents were amplified with an Axopatch 1C amplifier, filtered with an eight-pole low-pass Bessel filter (Frequency Devices, Haverhill, MA) at a cutoff frequency of 1 kHz, digitized at 5 kHz, and stored and analyzed on a Macintosh IIcx computer, using a GW Instruments MACAdios analog/digital converter and custom software written in our laboratory. Leak and capacitance correction was performed by digital summation of current recorded during 10–20-mV hyperpolarizing pulses, after appropriate scaling with current during depolarizing test pulses. All experiments were conducted at room temperature (20–22°).

Measurement of $[Ca^{2+}]_i$. $[Ca^{2+}]_i$ was determined using a microfluorimeter to monitor the Ca^{2+}-sensitive fluorescent chelator indo-1 (22). Cells were loaded with the dye by incubation in 2 μM indo-1/acetoxymethyl ester (Molecular Probes Inc., Eugene, OR), which is membrane permeant, for 45 min at 37°, in HEPES-buffered Hanks' balanced salt solution, pH 7.45, containing 0.5% bovine serum albumin. The HEPES-Hanks' solution was composed of the following (in mM): HEPES, 20; NaCl, 137; $CaCl_2$, 1.3; $MgSO_4$, 0.4; $MgCl_2$, 0.5; KCl, 5.4; KH_2PO_4, 0.4; $NaHPO_4$, 0.3; $NaHCO_3$, 3.0; and glucose, 5.6. After the loading incubation, during which time the dye ester was hydrolyzed by cytosolic esterases to the membrane-impermeant polycarboxylate anion that is indo-1, the cells were washed in the HEPES-Hanks' solution for 15 min.

Loaded and washed cells were mounted in a flow-through chamber for viewing (23). The superfusion chamber was mounted on an inverted microscope, and cells were localized by phase-contrast illumination. For excitation of the indo-1, the light from a 75-W xenon arc lamp was passed through a monochromator (Photon Technologies Inc., South Brunswick, NJ) set for 350 nm (slit width, 2 nm) and was collimated with a parabolic mirror. For epifluorescence, excitation light was reflected off a dichroic mirror (380 nm; Omega Optical, Brattleboro, VT) and through a 70× phase-contrast oil immersion objective (Leitz; numerical aperture, 1.15). Emitted light was sequentially reflected off dichroic mirrors (440 and 516 nm), through band-pass filters (405 ± 20 and 495 ± 20 nm, respectively), to photomultiplier tubes operating in photon-counting mode (Thorn EMI, Fairfield, NJ). Cells were illuminated with transmitted red light (610-nm long-pass) and visualized with a video camera placed after the second emission dichroic. Recordings were defined spatially with a rectangular diaphragm. The TTL photomultiplier output was integrated by passing the signal through an eight-pole Bessel filter at 2.5 Hz. This signal was then input into two channels of an analog/digital converter (Indec Systems, Sunnyvale, CA), sampling at 1 Hz. After completion of a given experiment, the microscope stage was adjusted so that no cells or debris occupied the field of view defined by the diaphragm, and then background light levels were determined (typically <5% of cell counts). Autofluoresence from cells that had not been loaded with indo-1 was not detectable. Records were later corrected for background and the ratios were recalculated. Ratios were converted to free $[Ca^{2+}]_i$ by using the equation $[Ca^{2+}]_i = K(R - R_{min})/(R_{max} - R)$, in which R is the 405/495-nm fluorescence ratio (22). The maximum ratio (R_{max}), the minimum ratio (R_{min}), and the constant K (product of the dissociation constant for indo-1 and the ratio of the free and bound forms of the dye at 495 nm) were determined from a standard curve to which the equation given above was fit using a nonlinear least-squares fit computer program. The system was recalibrated after any adjustment to the apparatus. Values for the constants R_{min}, R_{max}, and K ranged from 0.249 to 0.56, 1.91 to 4.11, and 1491 to 2712, respectively. The standard curve was determined from the indo-1 pentapotassium salt (20 μM) in calibration buffer (which was composed of, in mM, HEPES, 20; KCl, 127; NaCl, 10; and $MgCl_2$, 1; pH 7.1) containing 10 mM EGTA (stability constant = 3.969×10^6 M) (24) and varying amounts of added Ca^{2+}, which were calculated to give free Ca^{2+} concentrations ranging from 0 to 2000 nM. The validity of this calibration method was verified by determining R_{min} and R_{max} in ionomycin-permeabilized cells in Ca^{2+}-free buffer (1 mM EGTA) and saturating Ca^{2+} (10 mM Ca^{2+}).

All cells were continuously superfused with HEPES-Hanks', at a rate of 1.5 ml/min, for 15 min before start of an experiment. After selection of a suitable cell, defined as a rounded cell body that had extended fine processes and was isolated from other cells, basal $[Ca^{2+}]_i$ was recorded for 5 min and the superfusion was stopped for 7 min. Superfusion was then restarted and, after 1 min, a 50 mM K^+ depolarizing solution (in which K^+ was exchanged reciprocally for Na^+) was applied for 30 sec. Drugs were applied by superfusion for 2 min before stopping of the flow and were present in the depolarizing

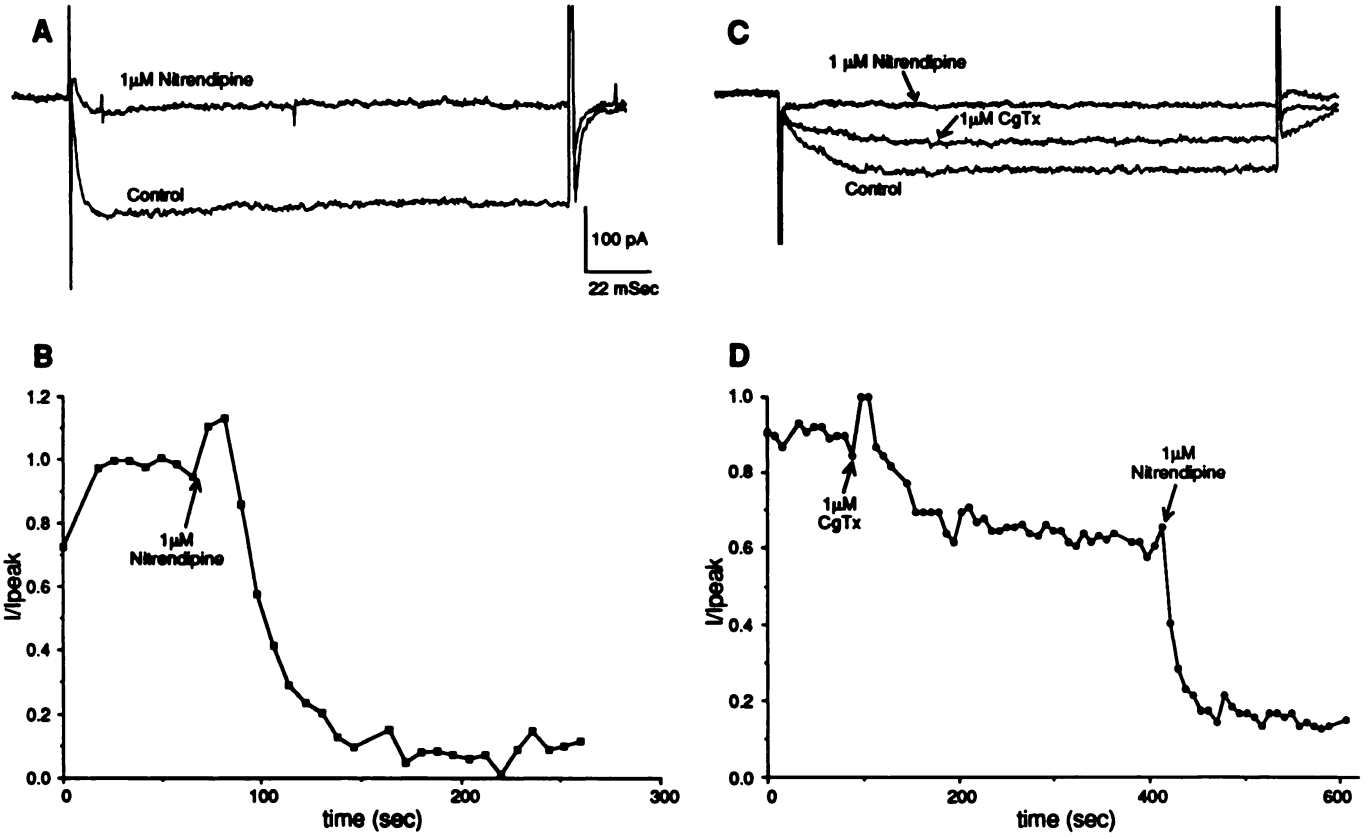

Fig. 1. ω-CgTx distinguishes two types of dihydropyridine-sensitive Ca^{2+} channels. Whole-cell Ca^{2+} currents were recorded in 5 mM Ba^{2+}, with all other ionic channels blocked by ionic substitution, as described in Materials and Methods. Test pulses (200 msec) to 0 mV were applied from a −30 mV holding potential. A and C, Representative sweeps taken from the plots shown below. B and D, Normalized peak inward current plotted versus time, with drug additions to the bathing media indicated by the *arrows*. Each plot is from an individual cell and is representative of two or three recordings.

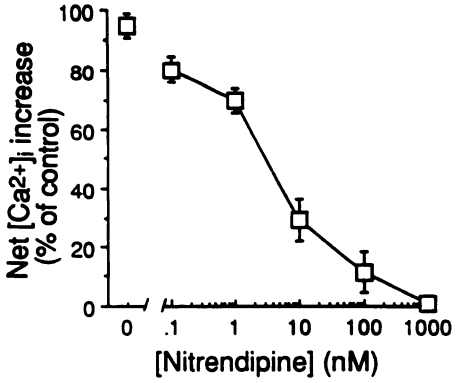

Fig. 2. Nitrendipine inhibits depolarization-induced $[Ca^{2+}]_i$ increases in a dose-dependent manner. Data are presented as mean ± standard error ($n \geq 3$), with each response in the presence of nitrendipine expressed as a percentage of the response before drug application. Note that 1000 nM nitrendipine completely blocks the rise in $[Ca^{2+}]_i$ (IC_{50} = 1.9 nM).

solution; thus, cells were preincubated with drugs for 10 min before the depolarizing stimulus. In some experiments, cells were exposed to drug for 30 min. In these studies, the superfusion was stopped for 27 min. In low-divalent cation solutions, Ca^{2+} and Mg^{2+} were reduced 10-fold, to 0.13 and 0.09 mM, respectively. Synthetic ω-CgTx was obtained from Sigma (St. Louis, MO), Calbiochem (San Diego, CA), Bachem (Torrance, CA), and Peninsula Laboratories (Belmont, CA), with similar results.

Results

NG108-15 cells were grown in serum-free, 5 μM forskolin-containing medium for 5–6 days, during which time the flat polygonal cells differentiated into rounded cells that extended fine processes and expressed voltage-sensitive Ca^{2+} channels. Whole-cell Ca^{2+} currents were recorded in 5 mM Ba^{2+}, with all other ionic currents blocked by ionic substitution, as described in Materials and Methods. Stepping to 0 mV from a holding potential of −30 mV elicited peak inward currents that ranged from 0.15 to 1 nA. The currents showed little inactivation over the course of the 200-msec test pulse (Fig. 1, A and C). Application of 1 μM nitrendipine inhibited the currents by 90% (n = 2) (Fig. 1, A and B). Thus, in NG108-15 cells most of the current elicited from this relatively positive holding potential is sensitive to dihydropyridine drugs. In contrast, 1 μM ω-CgTx inhibited the current by only 28% (n = 3), as shown in Fig. 1, C and D. Subsequent application of 1 μM nitrendipine reduced the remaining current by an additional 50% of the total current. Clearly, there are two nitrendipine-sensitive currents present in these cells; one is sensitive to ω-CgTx and the other is not. There was a small residual current that was neither ω-CgTx nor nitrendipine sensitive.

In order to further characterize the effects of ω-CgTx, we recorded depolarization-induced $[Ca^{2+}]_i$ transients in single cells, using dual-emission microfluorimetry and the Ca^{2+} indicator indo-1, as described in Materials and Methods. This technique allowed us investigate the effects of reduced extracellular divalent metals and prolonged exposures to ω-CgTx. These studies are not easily performed with the patch-clamp technique, because of signal to noise problems associated with reducing the concentration of the charge carrier and Ca^{2+}

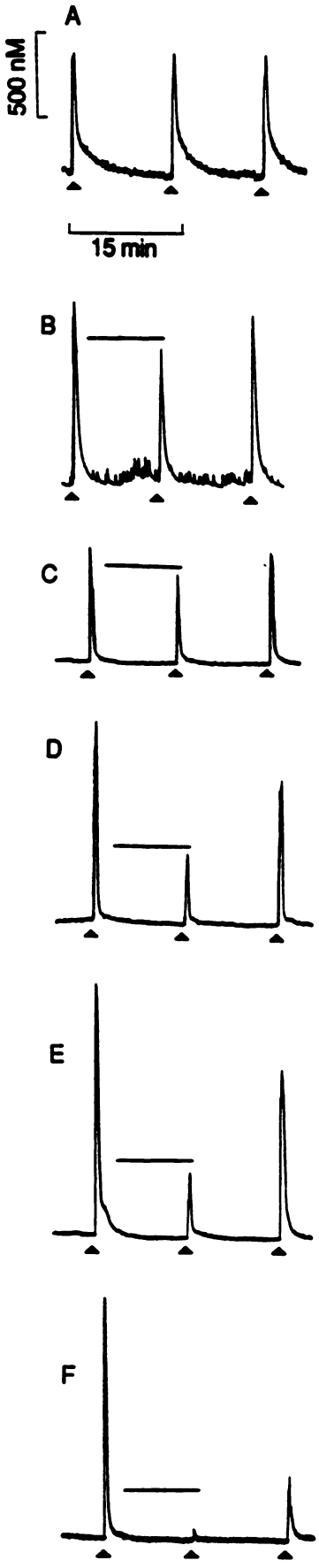

Fig. 3. Representative experimental records in the presence of nitrendipine. *Horizontal bars*, presence of various doses of nitrendipine (A, control; B, 0.1 nM; C, 1 nM; D, 10 nM; E, 100 nM; F, 1000 nM). ▲, Start of a 30-sec exposure to 50 mM K^+. Note that the $[Ca^{2+}]_i$ response partially recovers after removal of nitrendipine from the medium. Each record is from a different cell. All experiments were carried out in HEPES-Hanks' with normal divalent cation concentrations.

channel run down seen during long recordings. The average basal $[Ca^{2+}]_i$ was 142 ± 10 nM (n = 25), which is slightly higher than we have previously reported for neurons grown in primary culture (14). $[Ca^{2+}]_i$ transients were elicited by superfusion with a 50 mM K^+ depolarizing solution for 30 sec. This depolarization produced an average net $[Ca^{2+}]_i$ increase of 1513 ± 287 nM (n = 25), which was variable between cells but reproducible for a given cell. Thus, data are presented as a percentage of the pre-drug control response. Nitrendipine inhibited these depolarization-induced $[Ca^{2+}]_i$ transients in a dose-dependent manner, with an IC_{50} of 1.9 nM (Figs. 2 and 3). This finding is consistent with previous studies on these cells (25, 26). The effect was readily reversible (Fig. 3). This optical method for measuring Ca^{2+} influx is consistent with our results obtained with the whole-cell patch-clamp (Fig. 1). Depolarization by superfusion with 50 mM K^+ evokes responses that appear to be pharmacologically similar to currents elicited from the relatively positive holding potential of −30 mV, possibly because the depolarization occurs as a ramp during the approximately 10 sec needed to exchange the media bathing the cells.

In contrast to nitrendipine, ω-CgTx, at a maximally effective concentration of 100 nM, produced a 52% (n = 7) inhibition of the depolarization-induced $[Ca^{2+}]_i$ transient (Figs. 4 and 5). Interestingly, increasing the concentration of the peptide actually produced less inhibition. Indeed, supramaximal concentrations of the toxin produced a graded reduction in the attenuation of the $[Ca^{2+}]_i$ transient. This U-shaped dose-response curve was apparently mediated by the previously described ω-CgTx binding site (27–30), as indicated by the increased potency of the toxin when the divalent metal concentration was reduced. A 10-fold reduction in the extracellular Mg^{2+} and Ca^{2+} concentrations (to 0.09 and 0.13 mM, respectively) produced a 10-fold leftward shift in the dose-response curve, with no increase in the maximal effect. The entire curve, including the reversal of the effect, was shifted to lower toxin concentrations. In low-divalent cation media, depolarization evoked a net increase of 464 ± 63 nM from a resting $[Ca^{2+}]_i$ of 161 ± 12 nM (n = 21), which was smaller than the average response elicited in standard HEPES-Hanks' buffer.

Consistent with previous reports in other neuronal preparations, the inhibition produced by ω-CgTx was irreversible over the time course of our experiments (Figs. 5 and 8B) (11, 19). This finding is in contrast to the transient inhibition of L-type currents reported in the neuronal cell line PC12 (12). Note that nitrendipine-inhibited responses recovered significantly after washout of the drug (Fig. 3), in spite of the lipophilicity of this compound.

Because the occupancy of binding sites by irreversible ligands is determined by both the concentration and duration of ligand exposure, we explored the possibility that the maximal inhibition produced by ω-CgTx was limited by the duration of exposure. Increasing the duration of exposure from 10 to 30 min failed to increase the maximum inhibition of the depolarization-induced rise in $[Ca^{2+}]_i$ produced by ω-CgTx (Fig. 6). The longer incubation time (30 min) reduced the amplitude of the control responses. In cells that were stimulated every 5–15 min the responses were very consistent, but when cells remained

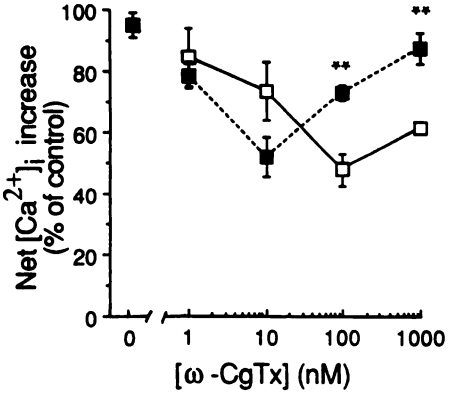

Fig. 4. ω-CgTx inhibits depolarization-induced increases in $[Ca^{2+}]_i$ in a concentration-dependent manner. ω-CgTx inhibits the rise in $[Ca^{2+}]_i$ in low-divalent cation (0.13 mM Ca^{2+}, 0.09 mM Mg^{2+}) (■) and normal (1.3 mM Ca^{2+}, 0.9 mM Mg^{2+}) (□) HEPES-Hanks'-based media, in a concentration-dependent manner. Data are presented as mean ± standard error ($n \geq 3$), with each response in the presence of ω-CgTx expressed as a percentage of the response before ω-CgTx application. **, Statistically significant differences ($p < 0.05$) between low and normal divalent cation conditions for the same concentration of ω-CgTx, as determined by Student's *t* test.

quiescent for 20–30 minutes, as was necessary for this series of experiments, the responses declined. The maximal inhibition produced by ω-CgTx, relative to this reduced control response, was 35%. The longer incubation time did shift the dose-response curve to the left, as would be expected for an irreversible agent. It appears that, in normal HEPES-Hanks' buffer, exposure to 100 nM ω-CgTx for 10 min maximally inhibits all of the Ca^{2+} channels that are sensitive to toxin in these cells.

These results suggest the presence of a population of dihydropyridine-sensitive, ω-CgTx-insensitive Ca^{2+} channels in NG108-15 cells. Indeed, when both drugs were sequentially applied to an individual cell, 1 μM nitrendipine completely abolished the remaining depolarization-induced $[Ca^{2+}]_i$ transient after a maximally effective dose of the toxin (100 nM) (Fig. 7).

In order to further characterize the action of ω-CgTx, cells were treated with the toxin repeatedly in low-divalent cation HEPES-Hanks' buffer. ω-CgTx (10 nM) inhibited the $[Ca^{2+}]_i$ response by approximately 45%, and this effect did not reverse significantly (Fig. 8B). A second exposure to 10 nM ω-CgTx produced no further inhibition of the $[Ca^{2+}]_i$ transient (Fig. 8C). This finding is consistent with the idea that there is a population of ω-CgTx-insensitive Ca^{2+} channels in these cells. When an exposure to 10 nM ω-CgTx was followed by exposure to 1000 nM ω-CgTx, no significant additional inhibition was observed, nor was there a reversal of the blockade, as might be predicted from the U-shaped dose-response curve (Fig. 8D). When the cell was first exposed to 1000 nM ω-CgTx, which had only minimal effects on the $[Ca^{2+}]_i$ response to 50 mM K^+, the cell was actually protected from a later exposure to the normally effective concentration of 10 nM (Fig. 8E). The high dose of ω-CgTx did not affect the ability of 1 μM nitrendipine to inhibit the increase in $[Ca^{2+}]_i$ (Fig. 8F), indicating that high concentrations of ω-CgTx do not simply mask the actions of Ca^{2+} channel blockers. Thus, the low affinity actions of ω-CgTx are apparently irreversible as well.

Discussion

The characterization of multiple types of Ca^{2+} channels in neurons (3, 4) and the subsequent discovery that individual

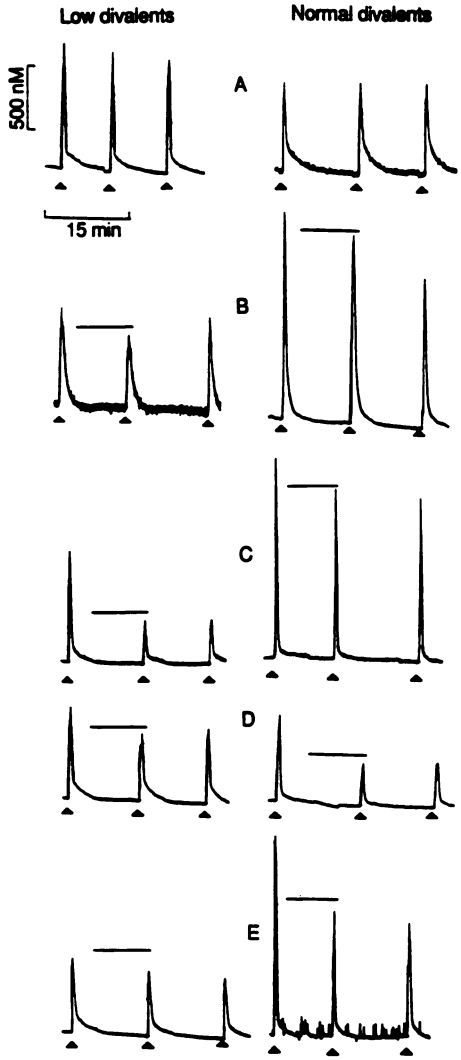

Fig. 5. ω-CgTx inhibits depolarization-induced $[Ca^{2+}]_i$ transients in normal and low divalent metal concentrations. Representative experimental records, each from a different cell, show the effects of various doses of ω-CgTx applied in the superfusion media, as indicated by the *horizontal bars* (A, control; B, 1 nM; C, 10 nM; D, 100 nM; E, 1000 nM). ▲, Beginning of a 30-sec exposure to 50 mM K^+. Note that there is no significant recovery of the $[Ca^{2+}]_i$ response after removal of ω-CgTx from the medium.

Ca^{2+} channel subtypes can be linked to specific neuronal functions (14) have provided a strong impetus to search for subtypes of Ca^{2+} channels and drugs that specifically target them. In this report, we have used pharmacological agents as tools to study Ca^{2+} channel subtypes in NG108-15 cells. Consistent with previous reports (25, 26), we have found that whole-cell Ba^{2+} currents elicited from −30 mV, as well as the entire depolarization-induced $[Ca^{2+}]_i$ transient in NG108-15 cells, are blocked by the dihydropyridine drug nitrendipine. However, only approximately half of this nitrendipine-sensitive Ca^{2+} influx was inhibited by ω-CgTx. The inhibition produced by ω-CgTx was concentration dependent, irreversible, and shifted to lower concentrations by decreases in the extracellular concentration of divalent metals, as previously described in radioligand binding experiments (27–30).

These results are significant in several respects. (i) ω-CgTx potently and irreversibly inhibits dihydropyridine-sensitive Ca^{2+} channels, and (ii) this inhibition is manifest in a U-shaped

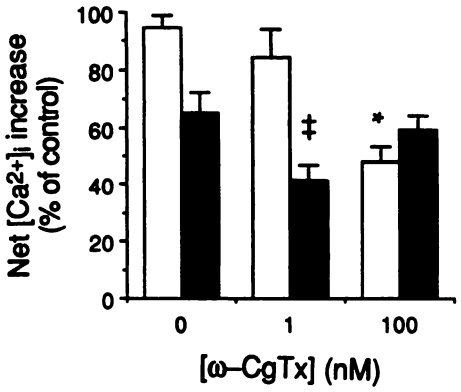

Fig. 6. Increasing the duration of exposure to ω-CgTx does not increase maximal inhibition. Exposing cells to ω-CgTx in normal HEPES-Hanks' (1.3 mM Ca^{2+}, 0.9 mM Mg^{2+}) for 30 min (■) shifts the dose-response curve to the left, compared with a 10-min exposure (□), without increasing the maximal effect. Data are presented as mean ± standard error ($n \geq 3$), expressed as percentage of pre-drug response. ‡, Significant difference ($p < 0.05$) from 30-min control; *, significant difference from 10-min control, as indicated by Student's t test.

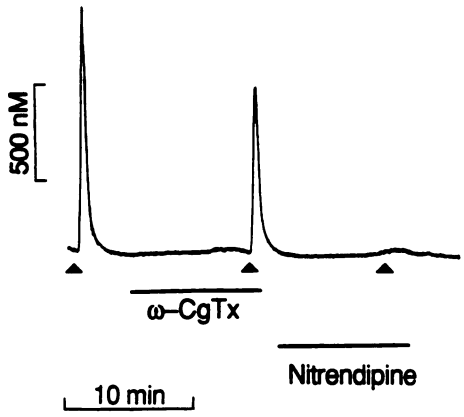

Fig. 7. Nitrendipine blocks residual depolarization-induced $[Ca^{2+}]_i$ response after application of ω-CgTx. The experimental trace shows partial blockade of the 50 mM K^+-induced $[Ca^{2+}]_i$ rise by a maximally effective concentration of 100 nM ω-CgTx. Nitrendipine (1 μM) blocks the remainder of this response. *Labeled bars*, drug presence; ▲, beginning of a 30-sec exposure to 50 mM K^+.

dose-response curve, showing inhibition of approximately 50% of the dihydropyridine-sensitive channels at a maximally effective concentration, suggesting that (iii) these cells contain two types of dihydropyridine-sensitive Ca^{2+} channels.

There is general agreement that ω-CgTx irreversibly blocks N-type neuronal Ca^{2+} channels. However, recent studies on another neuronal cell line, PC12 (12), and in chick sensory neurons (13) have suggested that there is a population of L-type channels that is unaffected or transiently blocked by ω-CgTx. We have demonstrated the presence of dihydropyridine-sensitive, ω-CgTx-insensitive channels in NG108-15 cells. Additionally, we have demonstrated unequivocally that dihydropyridine-sensitive, L-type Ca^{2+} channels can be irreversibly blocked by ω-CgTx. Furthermore, the U-shaped dose dependence of this effect may explain the controversy surrounding the action of this toxin on L-type channels. Studies in which ω-CgTx failed to inhibit L-type channels employed micromolar concentrations of the peptide, which, depending on the concentration of divalent metal ions, may prove ineffective, due to reversal of the Ca^{2+} channel blockade at higher ω-CgTx concentrations (12, 31).

There is precedence for an unusual dose dependence for ω-CgTx. Reynolds *et al.* (32) reported a dose-response curve for ω-CgTx in which the toxin maximally inhibited depolarization-induced $^{45}Ca^{2+}$ uptake in rat brain synaptosomes by 50%, with the effect gradually developing over 4 log units and with a plateau from 0.05 to 5 nM. In rat cerebellar cortex synaptosomes, Adamson *et al.* (33) found 93 nM ω-CgTx to be just as effective at inhibiting an increase in $[Ca^{2+}]_i$ as 1 μM ω-CgTx. Suszkiw *et al.* (34) reported a plateau in the dose-response curve of chick brain synaptosomes to ω-CgTx. These authors also reported that, in rat brain synaptosomes, only 40% of the total Ca^{2+} response was ω-CgTx sensitive. Similarly, Keith *et al.* (35) found that ω-CgTx inhibited only 55% of depolarization-induced [^{3}H]norepinephrine release. Thus, several reports suggest the presence, in neuronal tissue, of ω-CgTx-insensitive Ca^{2+} channels that are activated by protocols that would not be expected to recruit T-type channels.

Several possible explanations for the U-shaped dose response may be considered. Precipitation of ω-CgTx from solution at high concentrations seems unlikely, for several reasons. The peptide was diluted from a concentrated stock (100 μM), the concentration at which the effect began to reverse was only 100 nM, and the reversal was graded, with less block being produced as additional toxin was applied. Furthermore, pretreatment with a high (1 μM) concentration of ω-CgTx actually protected the channels from the effects of a subsequent exposure to 10 nM toxin. Finally, the entire U-shaped dose-response curve shifted in a parallel manner in response to changes in the extracellular divalent metal concentration. Divalent metals have been shown to regulate the ω-CgTx binding site in a similar fashion (27, 29, 30). Thus, it appears that the reversal of the toxin block is mediated through the ω-CgTx binding site. In order to further characterize the actions of ω-CgTx, Ca^{2+} influx was tested in a series of experiments in which ω-CgTx was applied sequentially to the same cell. ω-CgTx (10 nM) irreversibly inhibited the $[Ca^{2+}]_i$ increase by 45–50%. When applied a second time, 10 nM ω-CgTx had no detectable effect on the remaining Ca^{2+} response to 50 mM K^+. Application of 1 μM ω-CgTx, which alone produced no detectable alteration in the Ca^{2+} response, rendered 10 nM ω-CgTx ineffective at inhibiting the rise in $[Ca^{2+}]_i$. This finding suggests that, at higher peptide concentrations, ω-CgTx binds to a site that is ineffective at inhibiting Ca^{2+} influx but prevents ω-CgTx binding to the site that produces Ca^{2+} channel blockade. Once bound to this low affinity site, the effect does not readily reverse. This being the case, long incubations with low concentrations of ω-CgTx should produce the most effective inhibition of depolarization-induced Ca^{2+} influx. When cells were exposed to 1 or 100 nM ω-CgTx for 30 min, no increase in the maximal inhibition of the depolarization-induced rise in $[Ca^{2+}]_i$ was observed. This is consistent with the presence of two populations of dihydropyridine-sensitive Ca^{2+} channels in these cells.

There are a number of reports suggesting that additional Ca^{2+} channel subtypes may exist. In the PC12 cell line, an ω-CgTx-insensitive component of the N current has been described (12). Dihydropyridine-sensitive N channels have been reported in rat brainstem and spinal cord projection neurons (36), and ω-CgTx-insensitive, or partly sensitive, L-type channels have been described in chick sensory neurons (13, 31) and

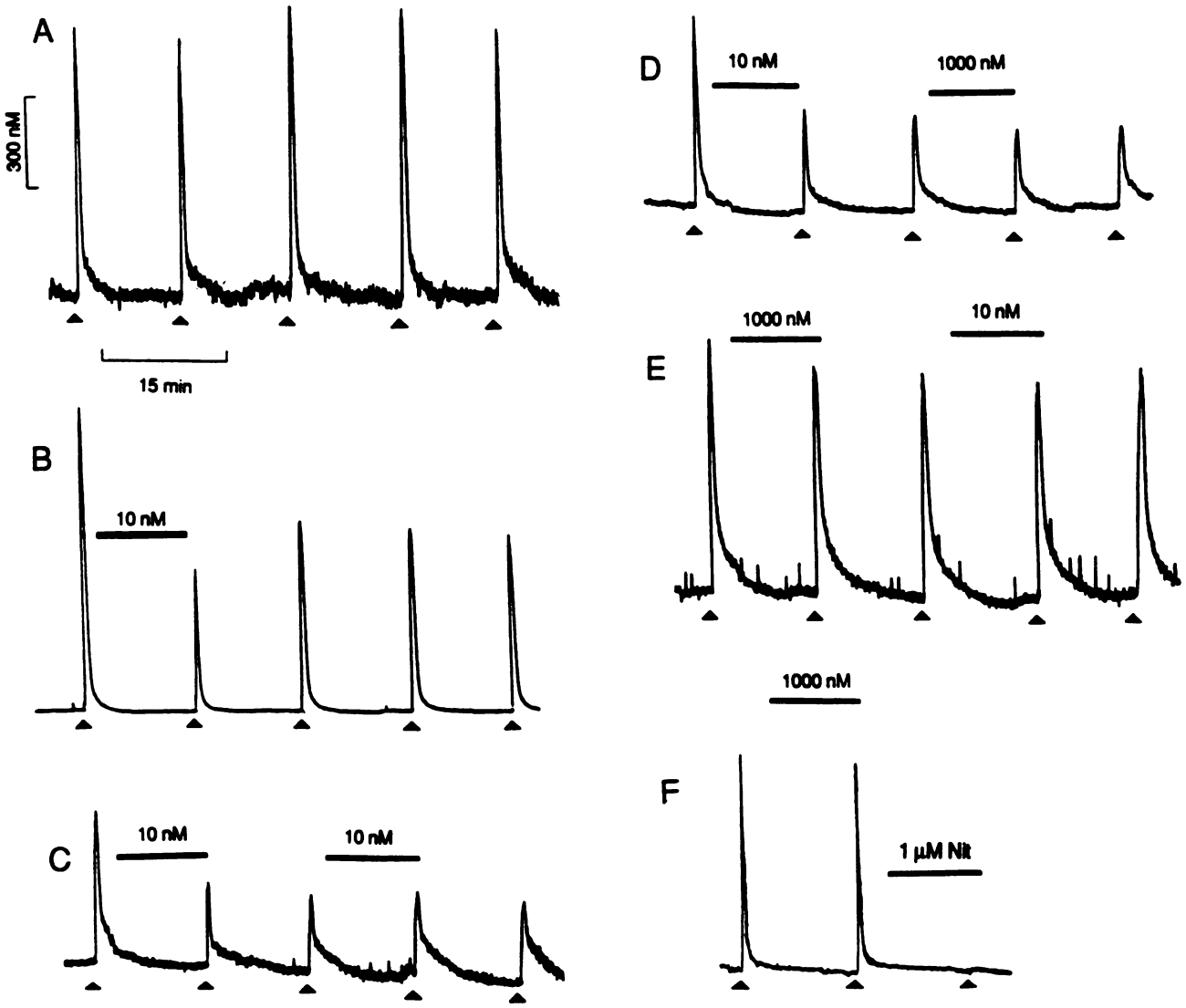

Fig. 8. Sequential application of various concentrations of ω-CgTx in low-divalent cation media. *Horizontal bars*, presence of ω-CgTx; ▲, start of a 30-sec exposure to 50 mM K^+. A, Control; B, 10 nM; C, 10 nM applied twice; D, 10 followed by 1000 nM; E, 1000 followed by 10 nM. F, Application of 1 μM ω-CgTx, which had very little effect on the depolarization-induced rise in $[Ca^{2+}]_i$, does not affect the blockade of this response by 1 μM nitrendipine (*Nit*). Each trace is representative of at least three experiments.

adrenal chromaffin cells (37). We have shown that, after a maximally effective concentration of ω-CgTx, the remaining depolarization-induced $[Ca^{2+}]_i$ transient can be blocked by nitrendipine (Figs. 1 and 7). These data indicate the presence of two populations of dihydropyridine-sensitive Ca^{2+} channels in the same cell, one blocked by ω-CgTx and the other resistant. Although the U-shaped dose-response curve produced by the toxin casts some doubt on this hypothesis, it is consistent with several experimental results. The maximal inhibition of approximately 50% could not be increased by (i) prolonged incubation time, (ii) decreased extracellular divalent metal concentrations, (iii) repeated exposure to ω-CgTx. We conclude that there are two populations of L-type channels coexpressed in a single cell. Because NG108-15 cells are a hybrid between a neuronal and a non-neuronal cell (neuroblastoma × glioma), it is possible that both neuronal (ω-CgTx-sensitive) and non-neuronal (ω-CgTx-insensitive) L-type channels are expressed. This scenario would suggest that the two channel types are structurally unique and that the differing pharmacological properties are not merely a result of the cellular environment.

In conclusion, we wish to suggest caution in the use of ω-CgTx as a tool for the pharmacological definition of Ca^{2+} channel subtypes. The toxin will clearly inhibit dihydropyridine-sensitive Ca^{2+} channels in an irreversible manner, but excessive concentrations of ω-CgTx actually render it ineffective in blocking Ca^{2+} channels. Furthermore, a dihydropyridine-sensitive, ω-CgTx-insensitive Ca^{2+} channel may be present in neuronal cells.

References

1. Miller, R. J. Multiple calcium channels and neuronal function. *Science (Washington D. C.)* **235**:46–52 (1987).
2. Carbone, E., and H. Lux. A low voltage-activated, fully inactivating Ca channel in vertebrate sensory neurones. *Nature (Lond.)* **310**:501–502 (1984).
3. Nowycky, M. C., A. P. Fox, and R. W. Tsien. Three types of neuronal calcium channel with different calcium agonist sensitivity. *Nature (Lond.)* **316**:440–443 (1985).
4. Fox, A. P., M. C. Nowycky, and R. W. Tsien. Kinetic and pharmacological

properties distinguishing three types of calcium currents in chick sensory neurones. *J. Physiol. (Lond.)* **394**:149–172 (1987).
5. Kostyuk, P. G., Y. M. Shuba, and A. N. Savchenko. Three types of calcium channels in the membrane of mouse sensory neurons. *Pflügers Arch.* **411**:661–669 (1988).
6. Llinas, R., M. Sugimori, J.-W. Lin, and B. Cherksey. Blocking and isolation of a calcium channel from neurons in mammals and cephalopods utilizing a toxin fraction (FTX) from funnel-web spider poison. *Proc. Natl. Acad. Sci. USA* **86**:1689–1693 (1989).
7. Tang, C., F. Presser, and M. Morad. Amiloride selectively blocks the low threshold (T) calcium channel. *Science (Washington D. C.)* **240**:213–215 (1988).
8. Olivera, B. M., J. Rivier, C. Clark, C. A. Ramilo, G. P. Corpuz, F. C. Abogadie, E. E. Mena, S. R. Woodward, D. R. Hillyard, and L. J. Cruz. Diversity of *Conus* neuropeptides. *Science (Washington D. C.)* **249**:257–263 (1990).
9. de Weille, J. R., H. Schweitz, P. Maes, A. Tartar, and M. Lazdunski. Calciseptin, a peptide isolated from black mamba venom, is a specific blocker of the L-type calcium channel. *Proc. Natl. Acad. Sci. USA* **88**:2437–2440 (1991).
10. Callewaert, G., I. Hanbauer, and M. Morad. Modulation of calcium channels in cardiac and neuronal cells by an endogenous peptide. *Science (Washington D. C.)* **243**:663–666 (1989).
11. McCleskey, E. W., A. P. Fox, D. Feldman, L. J. Cruz, B. M. Olivera, R. W. Tsien, and D. Yoshikami. Calcium channel blockade by a peptide from *Conus*: specificity and mechanism. *Proc. Natl. Acad. Sci. USA* **84**:4327–4331 (1987).
12. Plummer, M. R., D. E. Logothetis, and P. Hess. Elementary properties and pharmacological sensitivities of calcium channels in mammalian peripheral neurons. *Neuron* **2**:1453–1463 (1989).
13. Aosaki, T., and H. Kasai. Characterization of two kinds of high-voltage-activated Ca-channel currents in chick sensory neurons: differential sensitivity to dihydropyridines and *omega*-conotoxin GVIA. *Pflügers Arch.* **414**:150–156 (1989).
14. Hirning, L. D., A. P. Fox, E. W. McCleskey, B. M. Olivera, S. A. Thayer, R. J. Miller, and R. W. Tsien. Dominant role of N-type Ca channels in evoked release of norepinephrine from sympathetic neurons. *Science (Washington D. C.)* **239**:57–60 (1988).
15. Perney, T. M., L. D. Hirning, S. E. Leeman, and R. J. Miller. Multiple calcium channels mediate neurotransmitter release from peripheral neurons. *Proc. Natl. Acad. Sci. USA* **83**:6656–6659 (1986).
16. Holz, G. G., K. Dunlap, and R. M. Kream. Characterization of the electrically evoked release of substance P from dorsal root ganglion neurons: methods and dihydropyridine sensitivity. *J. Neurosci.* **8**:463–471 (1988).
17. Llinas, R. R. The intrinsic electrophysiological properties of mammalian neurons: insights into central nervous system function. *Science (Washington D. C.)* **242**:1654–1664 (1988).
18. Tank, D. W., M. Sugimori, J. A. Connor, and R. R. Llinas. Spatially resolved calcium dynamics of mammalian Purkinje cells in cerebellar slice. *Science (Washington D. C.)* **242**:773–778 (1988).
19. Kerr, L., and D. Yoshikami. A venom peptide with a novel presynaptic blocking action. *Nature (Lond.)* **308**:282–284 (1984).
20. Law, P. Y., J. E. Koehler, and H. H. Loh. Comparison of opiate inhibition of adenylate cyclase activity in neuroblastoma N18TG2 and neuroblastoma × glioma NG108-15 hybrid cell lines. *Mol Pharmacol.* **21**:483–491 (1981).
21. Hamill, O. P., A. Marty, E. Neher, B. Sakmann, and F. Sigworth. Improved patch-clamp techniques for high resolution current recording from cells and cell-free membrane patches. *Pflügers Arch. Eur. J. Physiol.* **391**:85–100 (1981).
22. Grynkiewicz, G., M. Peonie, and R. Y. Tsien. A new generation of Ca^{2+} indicators with greatly improved fluorescence properties. *J. Biol. Chem.* **260**:3440–3450 (1985).
23. Thayer, S. A., M. Sturek, and R. J. Miller. Measurement of neuronal Ca^{2+} transients using simultaneous microfluorimetry and electrophysiology. *Pflügers Arch. Eur. J. Physiol.* **412**:216–223 (1988).
24. Fabiato, A., and F. Fabiato. Calculator programs for computing the composition of the solutions containing multiple metals and ligands used for experiments in skinned muscle cells. *J. Physiol. (Paris)* **75**:463–505 (1979).
25. Freedman, S. B., G. Dawson, M. L. Villereal, and R. J. Miller. Identification and characterization of voltage-sensitive calcium channels in neuronal clonal cell lines. *J. Neurochem.* **4**:1453–1467 (1984).
26. Tsunoo, A., M. Yoshii, and T. Narahashi. Block of calcium channels by enkephalin and somatostatin in neuroblastoma-glioma hybrid NG108-15 cells. *Proc. Natl. Acad. Sci. USA* **83**:9832–9836 (1986).
27. Cruz, L. J., and B. M. Olivera. Calcium channel antagonists: *omega*-conotoxin defines a new high affinity site. *J. Biol. Chem.* **261**:6230–6233 (1986).
28. Wagner, J. A., A. M. Snowman, A. Biswas, and S. H. Snyder. ω-Conotoxin GVIA binding to a high affinity receptor in brain: characterization, calcium sensitivity and solubilization. *J. Neurosci.* **8**:3354–3359 (1988).
29. Abe, T., K. Koyano, H. Saisu, Y. Nishiuchi, and S. Sakakibara. Binding of *omega*-conotoxin to receptor sites associated with the voltage-sensitive calcium channel. *Neurosci. Lett.* **71**:203–208 (1986).
30. Sher, E., A. Pandiella, and F. Clementi. ω-Conotoxin binding and effects on calcium channel function in human neuroblastoma and rat pheochromocytoma cell lines. *FEBS Lett.* **235**:178–182 (1988).
31. Kasai, H., T. Aosaki, and J. Fukuda. Presynaptic Ca-antagonist *omega*-conotoxin irreversibly blocks N-type Ca-channels in chick sensory neurons. *Neurosci. Res.* **4**:228–235 (1987).
32. Reynolds, I. J., J. A. Wagner, S. H. Snyder, S. A. Thayer, B. M. Olivera, and R. J. Miller. Brain voltage-sensitive calcium channel subtypes differentiated by ω-conotoxin fraction GVIA. *Proc. Natl. Acad. Sci. USA* **83**:8804–8807 (1986).
33. Adamson, P., J. Z. Xiang, T. Mantzourides, M. J. Brammer, and I. C. Campbell. Presynaptic *alpha*$_2$-adrenoceptor and *kappa*-opiate receptor occupancy promotes closure of neuronal (N-type) calcium channels. *Eur. J. Pharmacol.* **174**:63–70 (1989).
34. Suszkiw, J., M. Murawsky, and R. Fortner. Heterogeneity of presynaptic calcium channels revealed by species differences in the sensitivity of synaptosomal ^{45}Ca entry to *omega*-conotoxin. *Biochem. Biophys. Res. Commun.* **145**:1283–1286 (1987).
35. Keith, R. A., T. J. Mangano, M. A. Pacheco, and A. I. Salama. Characterization of the effects of ω-conotoxin GVIA on the responses of voltage-sensitive calcium channels. *J. Auton. Pharmacol.* **9**:243–252 (1989).
36. Huang, L. M. Calcium channels in isolated rat dorsal horn neurones, including labelled spinothalamic and trigeminothalamic cells. *J. Physiol. (Lond.)* **411**:161–177 (1989).
37. Owen, P., D. Marriott, and M. Boarder. Evidence for a dihydropyridine-sensitive and conotoxin-insensitive release of noradrenaline and uptake of calcium in adrenal chromaffin cells. *Br. J. Pharmacol.* **97**:133–138 (1989).

Send reprint requests to: S. A. Thayer, Department of Pharmacology, University of Minnesota Medical School, 3-249 Millard Hall, 435 Delaware Street S.E., Minneapolis, MN 55455.